

# Nonexistent electron affinity of OCS and the stabilization of carbonyl sulfide anions by gas phase hydration

Eric Surber, S. P. Ananthavel, and Andrei Sanov<sup>a)</sup>

*Department of Chemistry, University of Arizona, Tucson, Arizona 85721-0041*

(Received 17 September 2001; accepted 14 November 2001)

We report the formation of heterogeneous OCS–water cluster anions  $[(\text{OCS})_n(\text{H}_2\text{O})_k]^-$  ( $n \geq 1, n + k \geq 2$ ), of which  $\text{OCS}^- \cdot \text{H}_2\text{O}$  is the most interesting species in view of the near absence of unhydrated  $\text{OCS}^-$  in the same ion source. The presence of  $\text{OCS}^- \cdot \text{H}_2\text{O}$  indicates that the intra-cluster formation of  $\text{OCS}^-$  does occur as part of the  $[(\text{OCS})_n(\text{H}_2\text{O})_k]^-$  formation mechanism. In this light, the near absence of unhydrated  $\text{OCS}^-$  anions points towards their metastable nature, while the abundance of the hydrated anions is attributed to the stabilizing effect of hydration. These conclusions are supported by the results of an extensive theoretical investigation of the adiabatic electron affinity (EA) of OCS. We conclude that the EA of OCS is either negative or essentially zero. The best estimate based on the Gaussian-3 theory calculation puts the EA at  $-0.059 \pm 0.061$  eV. A study of the structure and energetics of  $\text{OCS}^- \cdot \text{H}_2\text{O}$  predicts the existence of four structural isomers. Using the coupled-cluster theory, we find that the most stable structure is stabilized by 0.543 eV relative to the separated  $\text{OCS}^- + \text{H}_2\text{O}$  limit. © 2002 American Institute of Physics. [DOI: 10.1063/1.1433001]

## I. INTRODUCTION

Solvation is known to have a dramatic effect on the energetic and structural properties of gas-phase anions. Particularly interesting are the cases in which the corresponding neutral molecule has no electron affinity, yet the anion can be stabilized and studied within a cluster. The strong ion–neutral interactions lower the energy of the cluster anion relative to the neutral state and can even lead to the formation of new chemical bonds.

Important cases in point are the  $(\text{CO}_2)_n^-$  and  $(\text{OCS})_n^-$  cluster anions. One fundamental question regarding these clusters, as well as the isovalent  $(\text{CS}_2)_n^-$ , is whether the excess electron is localized on a single monomer or shared between two (or more) monomer moieties.<sup>1–9</sup> The closed-shell  $\text{CO}_2$  molecule has no electron affinity,<sup>10</sup> and  $\text{CO}_2^-$  is not stable as an isolated species. Small amounts of  $\text{CO}_2^-$  can be observed in the gas phase under certain ion source conditions,<sup>3,6,11</sup> as the metastable anion owes its limited existence ( $< 100 \mu\text{s}$ )<sup>10,12,13</sup> to the potential barrier separating its bent equilibrium from the linear region of the adiabatic potential, which corresponds to the autodetached state. On the other hand, since the early work of Klots and Compton<sup>14</sup> it is known that homogeneous  $(\text{CO}_2)_n^-$  cluster anions can be prepared by low-energy electron attachment to neutral clusters.<sup>2–7,15–25</sup> It is also known that the excess electron localizes on a single  $\text{CO}_2$  molecule only within the cluster size range from  $n=7$  to 13, while in smaller ( $n < 6$ ) and larger ( $n > 13$ ) clusters the dimer structure of the anionic core predicted by Fleischman and Jordan<sup>8</sup> is favored.<sup>3,4</sup> Thus, the  $\text{CO}_2^-$  anion exists within a cluster only if certain solvent coordination requirements are met. In other cases, a molecu-

lar rearrangement following the electron attachment leads to the formation of a new chemical bond and a more stable dimer anion core.<sup>8</sup> Small anionic clusters of  $\text{CS}_2$  ( $n \leq 4$ ) have also been shown to have a dimer core structure,<sup>2,7,26</sup> even though  $\text{CS}_2$  has positive electron affinity<sup>10,27,28</sup> and the coexistence of isomers with the dimer and monomer anion cores has not been ruled out.<sup>5</sup>

While  $(\text{CO}_2)_n^-$  and  $(\text{CS}_2)_n^-$  have been the subject of several experimental<sup>2–7,14–25</sup> and theoretical<sup>2,7,8,26</sup> studies, much less is known about the anions of carbonyl sulfide.<sup>9,22,28</sup> In several important respects, the molecular and cluster anions of OCS bridge the gap between the energetic and structural properties of  $(\text{CO}_2)_n^-$  and  $(\text{CS}_2)_n^-$ . Yet even such fundamental property, as the value of adiabatic electron affinity (EA) of OCS, has remained unclear. As with  $\text{CO}_2$  and  $\text{CS}_2$ , an experimental measurement is complicated by the significant mismatch between the equilibrium geometries of the neutral and the anion. While for  $\text{CO}_2$  (EA =  $-0.6$  eV)<sup>10</sup> and  $\text{CS}_2$  (EA =  $0.9–1.0$  eV)<sup>10,27</sup> at least the *sign* of the EA presents no doubt, even such qualitative certainty is not available for OCS. Since the properties of OCS are intermediate between those of  $\text{CO}_2$  and  $\text{CS}_2$ , its EA is close to zero, making its careful determination crucial for a description of the stability and other properties of carbonyl sulfide anions.

The only experimental measurement of the EA of OCS reported in the literature places it at  $0.46 \pm 0.2$  eV.<sup>10,29</sup> However, this result is difficult to reconcile with the observed absence of the  $\text{OCS}^-$  monomer anions in the  $(\text{OCS})_n^-$  family.<sup>9</sup> It is also inconsistent with the theoretical study by Gutsev *et al.*, who predicted the EA to be  $-0.22$  eV at the CCSD(T) level.<sup>28</sup> In this publication, we reinforce the indirect experimental evidence that  $\text{OCS}^-$  is metastable. In addition, we report the most extensive to-date theoretical investigation of the EA of OCS, which leads us to conclude, *with*

<sup>a)</sup> Author to whom correspondence should be addressed. Electronic mail: sanov@u.arizona.edu

quantifiable confidence, that the EA is either slightly negative or essentially zero.

The absence of  $\text{OCS}^-$  in the  $(\text{OCS})_n^-$  ion beam is only an indirect indication that OCS has no electron affinity. The appearance of  $\text{OCS}^-$  fragments (with a lifetime  $\geq 5 \mu\text{s}$ ) resulting from the photodissociation of  $(\text{OCS})_n^-$  is another piece of the puzzle,<sup>9</sup> suggesting a metastable (rather than unstable) nature of  $\text{OCS}^-$ . These observations are inconclusive, because the absence of the monomers in the  $(\text{OCS})_n^-$  ion beam could also be explained by the mechanism of formation of  $(\text{OCS})_n^-$  clusters rather than the  $\text{OCS}^-$  energetics.

The likely mechanism of  $(\text{OCS})_n^-$  formation involves the attachment of slow electrons to neutral clusters of OCS, followed by the cluster cooling<sup>30</sup> via the loss of solvent molecules and subsequent growth of a solvent shell via the long-range ion–neutral interactions in the supersonic expansion.<sup>31</sup> An isolated OCS molecule could not capture an electron even if it had slightly positive adiabatic EA, because of the geometry difference between the linear OCS and bent  $\text{OCS}^-$  equilibria. Since there is clear evidence of the existence of the covalently bound  $(\text{OCS})_2^-$  cluster core,<sup>9</sup> it is possible that the formation of small  $(\text{OCS})_n^-$  cluster ions *always* involves a molecular rearrangement leading to the stable dimer core. In this case, the monomer  $\text{OCS}^-$  anions would not be formed because the solvent loss stops at the dimer level, not because  $\text{OCS}^-$  is unstable.

The structural properties of cluster ions can change dramatically with the addition of heterogeneous solvent molecules. For example, the hydrated  $(\text{CO}_2)_n^-$  clusters are characterized by the coexistence of electronic isomers with the  $\text{CO}_2^-$  and  $(\text{CO}_2)_2^-$  cluster cores,<sup>11</sup> contrary to the homogeneous  $(\text{CO}_2)_n^-$  cluster ions, in which only the dimer core structure was detected in the  $2 \leq n \leq 5$  size range.<sup>3,4</sup> This effect of heterogeneous solvation opens a way for preparing the monomer anions within small heterogeneous clusters.

In this paper, we report for the first time the formation of heterogeneous OCS–water cluster anions  $[(\text{OCS})_n(\text{H}_2\text{O})_k]^-$ . We focus mainly on the monohydrated monomer anion ( $n=k=1$ ), whose structure is described as  $\text{OCS}^- \cdot \text{H}_2\text{O}$ . Its presence indicates that the  $[(\text{OCS})_n(\text{H}_2\text{O})_k]^-$  dynamics do lead to the intra-cluster formation of the  $\text{OCS}^-$  monomers. In this light, the near absence of the unhydrated  $\text{OCS}^-$  anions produced via the same mechanism cannot be explained by the dimer core formation and points towards the instability of  $\text{OCS}^-$  in the absence of the stabilizing effect of hydration.

The details of the experimental and theoretical methods employed in this study are given in Sec. II. The experimental results are presented in Sec. III. In Sec. IV, we report a theoretical investigation of the adiabatic EA of OCS, followed by a study of  $\text{OCS}^- \cdot \text{H}_2\text{O}$  structure and energetics. Section V summarizes the conclusions and outlines the future experimental directions.

## II. EXPERIMENTAL AND COMPUTATIONAL METHODS

### A. Experimental setup

The experiments were carried out during the initial testing of the ion delivery components of a new negative-ion

photoelectron imaging spectrometer. The complete details of the apparatus will be given in forthcoming publications. In brief, the apparatus consists of a pulsed ion source, a time-of-flight (TOF) ion mass-spectrometer, and a photoelectron imaging assembly. Only the first two components are used in the present study.

The ion source and the mass-spectrometer conform to the state of art developed by Lineberger and co-workers.<sup>31,32</sup> The negative ions are formed and cooled in an electron-impact ionized pulsed supersonic expansion.<sup>31</sup> A room-temperature mixture of 7% OCS in Ar with trace amount of water is expanded into the ion source chamber (base pressure of  $< 10^{-6}$  Torr) through a pulsed supersonic valve (General Valve Series 9) operated with a backing pressure of 1.5 atm at a repetition rate of 50 Hz. The home-built driver for the valve is based on the circuit design provided by Kukolich.<sup>33</sup> About 1 to 2 mm from the 500  $\mu\text{m}$  diameter nozzle orifice the expansion is crossed with a well controlled  $\sim 100 \mu\text{A}$  beam of electrons from a home-built 1 keV electron gun. The 1 keV electrons ionize the expansion, giving rise to slow secondary electrons, which in turn attach to the neutral clusters, and thus the negative ions are formed.

About 15 cm downstream from the nozzle, the anions are pulse-extracted into the 1.7 m long Wiley–McLaren TOF mass spectrometer.<sup>34</sup> The repeller plate is driven by a 10 ns rise–fall-time high-voltage pulse generator (model PVM-4210, Directed Energy, Inc.). The amplitude of the extraction pulse is adjusted for optimum Wiley–McLaren focusing, the typical value being about  $-600$  V. The ions pass through a 4 mm diameter orifice in the grounded electrode, serving as a partition between the source chamber and the rest of the instrument, and enter the acceleration stack, where a uniform electric field from ten evenly spaced electrodes accelerates them to the 1950 V beam potential.

The beam of accelerated ions is steered and focused using electrostatic deflectors and an Einzel lens. The ions are referenced from the original 1950 V beam potential down to the ground potential without affecting their kinetic energy using a fast Johnson-type potential switch.<sup>35</sup> The switch is a 60 cm long, 7.5 cm diameter stainless steel tube with apertures at both ends, driven by a 25 ns rise–fall-time high-voltage pulse generator (model PVX-4140, Directed Energy, Inc.). The ions of interest enter the tube while it is at 1950 V. Once the ions are inside, the tube's potential is dropped to 0 V, with the ions experiencing no field from the switch at any time. The delay of the potential switch trigger relative to the ion extraction pulse controls the mass range of the ions that pass through the switch unabated, while the physical length of the tube determines the width of the working mass range.

After passing through two more differentially pumped regions and a series of apertures, the ions enter the detection chamber with a base pressure of which rises  $\sim 3 \times 10^{-9}$  Torr, rising slightly during the experiment, when the gate valve connecting the detection chamber with the rest of the instrument is opened. The ions are detected at the temporal and spatial focus of the mass-spectrometer using a Chevron type dual microchannel plate (MCP) detector (25 mm diam. plates) from Burle, Inc. Before impacting the detector, the ions are post-accelerated by additional 1 kV, in-

creasing their kinetic energy to  $>3$  kV. The electrons formed inside the MCPs (bias 700–800 V per plate) are collected by a metal anode biased by additional 200 V. The signal from the anode riding on top of a high-voltage pedestal is capacitively coupled down to the ground potential, amplified by a 100 MHz,  $100\times$  amplifier (Phillips Scientific), and averaged (typically, for 512 cycles at a time) using a 300 MHz, 2.5 Gsamples/second digital oscilloscope (Tektronix TDS 3032).

The anion TOF spectra are converted into mass spectra by first relying on the calibration of the mass spectrometer based on the known experimental parameters. The exact assignment is achieved by choosing pairs of prominent peaks with unambiguous preliminary assignments, and adjusting the flight-time to mass conversion parameters to satisfy the chosen time-mass pairs.

## B. Computational details

The calculations are carried out with the GAUSSIAN 98 suite of programs,<sup>36</sup> employing a range of *ab initio* and hybrid Hartree–Fock density functional theory (DFT) methods with two classes of basis sets: The split-valence sets of Pople with added diffuse and polarization functions [6-31+G(*d,p*), 6-311+G(*d,p*), and others], and the augmented correlation-consistent basis sets of Dunning (aug-cc-pVXZ, where X=D, T, Q, for double, triple, and quadruple- $\zeta$ ). The new G3large basis set [an improved version of 6-311+G(3*df*,2*p*) with modified polarization functions]<sup>37</sup> was also used in some calculations.

The *ab initio* calculations were carried out using several methods accounting for electron correlation: the Møller–Plesset perturbation theory,<sup>38</sup> the coupled-cluster theory,<sup>39,40</sup> and the nonvariational quadratic configuration interaction (CI) method.<sup>41</sup> The Møller–Plesset correlation energy correction was computed to the second,<sup>42–44</sup> third,<sup>43,45</sup> and fourth<sup>46</sup> orders (MP2, MP3, and MP4, respectively). The fourth-order Møller–Plesset calculations were complete with single, double, triple, and quadruple substitutions (MP4-SDTQ). The coupled-cluster theory and quadratic CI calculations included single and double excitations, with triple excitations treated perturbatively, where indicated [CCSD, CCSD(T), and QCISD(T)].<sup>41,47–49</sup>

The EA of OCS was also determined using the Gaussian-2 (G2)<sup>50</sup> and Gaussian-3 (G3) composite theories using a series of *ab initio* calculations plus empirical corrections.<sup>37</sup> The principal reason why the Gaussian theories are attractive for this study is that their performance in calculating the total energies and EAs has been thoroughly tested on the sets of experimental data known as the G2/97<sup>51,52</sup> and G3/99<sup>53</sup> test sets. The availability of published test data statistics<sup>37,52</sup> enables us to assign meaningful margins of trust to the computed EA values. The G3 theory performs well for small systems<sup>37,52</sup> and thus its application to OCS is justified. The final G2 and G3 energies are effectively at the QCISD(T) level with the 6-311+G(3*df*) and G3 large basis sets, respectively,<sup>37,50</sup> with the high-level accuracy achieved at significantly lower computational cost than that of a direct calculation.

The computational steps comprising the G2 and G3 methods were carried out with GAUSSIAN 98 and the neces-

sary energy corrections were combined to yield the total energies of OCS and OCS<sup>-</sup> at 0 K, referred to as the G2 and G3 energies.<sup>37</sup> The neutral OCS molecule is in the G2/97 test set.<sup>37</sup> However, to the best of our knowledge, the G3 energy of OCS<sup>-</sup> has not been calculated previously. Since the zero-point vibrational energy is included in the G2 and G3 energies, the corresponding adiabatic EAs were directly determined as the difference between the  $G_n$  energies of the neutral and the anion.

The DFT was chosen for its computational efficiency, which is particularly important for the cluster ion calculations, as well as for its track record in predicting electron affinities.<sup>54</sup> The specific DFT methods used in this study are BLYP, B3LYP, and *m*PW1PW. The first two employ the 1988 functional<sup>55</sup> and the three-parameter exchange functional<sup>56</sup> of Becke, respectively, in conjunction with the correlation functional of Lee, Young, and Parr.<sup>57</sup> The *m*PW1PW method is based on Barone and Adamo's Becke-style one-parameter hybrid functional with modified Perdew–Wang exchange and correlation and improved long-range behavior.<sup>58</sup>

The spin-unrestricted methods were used for open-shell systems, while spin-restricted calculations were carried out in the closed-shell cases. By default, only the outer-shell electrons were included in the correlation calculations. However, in several cases (identified by the “full” keyword), full correlation calculations were carried out in order to quantify the effect of including the inner-shell electrons. For geometry optimizations, the Berny algorithm<sup>59</sup> was used by default. In calculations on some cluster ion conformations involving rather flat potential energy surfaces, the conversion was achieved using the modified GDIIS method (geometry by direct inversion in the iterative subspace).<sup>60</sup>

## III. EXPERIMENTAL RESULTS

Figure 1 shows the negative ion mass spectra obtained with the OCS–Ar precursor containing a trace of water. The spectra in Figs. 1(a)–1(c) were recorded at different delays between the ion extraction pulse and the potential switch trigger: 11.8, 13.6, and 26.6  $\mu$ s, respectively. In each case, the focusing was optimized for the particular mass range. The magnified spectrum in Fig. 1(a) was optimized for the S<sup>-</sup> anions; it demonstrates the accuracy of our calibration. The most prominent S<sup>-</sup> peak corresponds to the <sup>32</sup>S<sup>-</sup> isotope, with the largest satellite peak assigned to <sup>34</sup>S<sup>-</sup> (natural abundances of 95.02% and 4.21%, respectively).<sup>29</sup> Signal due to <sup>33</sup>S<sup>-</sup> 0.75%<sup>29</sup> is also discernable.

The most intense peaks in both Figs. 1(a) and 1(b) correspond to S<sub>2</sub><sup>-</sup>. Since a single precursor molecule contains only one sulfur atom, the S<sub>2</sub><sup>-</sup> anions must be formed from clusters of OCS. There is no ambiguity in assigning this peak to S<sub>2</sub><sup>-</sup> ( $m=64$ ), rather than OCS<sup>-</sup> ( $m=60$ ). Our confidence is reinforced by the satellite peak at  $m=66$ , assigned to <sup>32</sup>S<sup>34</sup>S<sup>-</sup>, whose relative intensity is in agreement with the expected abundance ratio of <sup>32</sup>S<sup>34</sup>S<sup>-</sup> and <sup>32</sup>S<sub>2</sub><sup>-</sup> (0.08).

We observe almost no signal at  $m=60$ , corresponding to OCS<sup>-</sup>. The barely measurable  $m=60$  signal was found to be dependent on the supersonic expansion conditions and par-

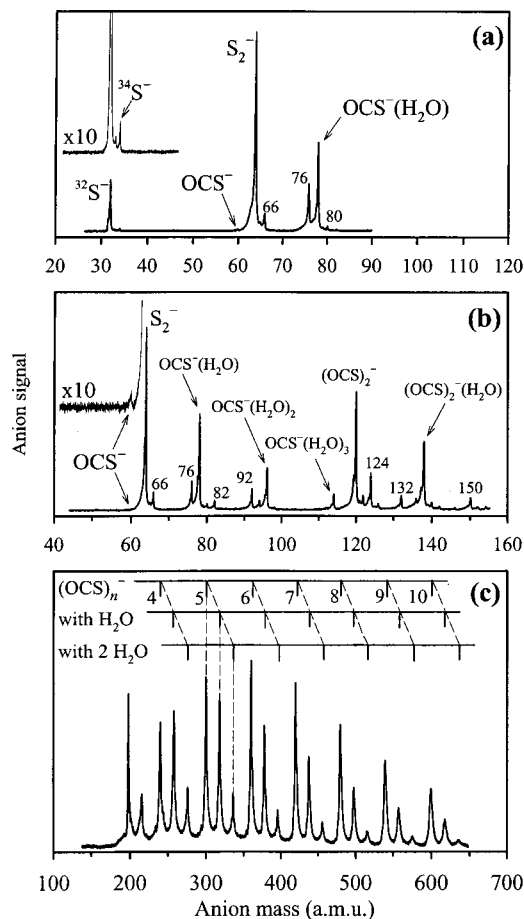


FIG. 1. Negative ion mass spectra obtained with the OCS–Ar precursor containing a trace amount of water. The magnified ( $\times 10$ ) spectra in (a) and (b) correspond to experimental conditions optimized for the  $S^-$  and  $OCS^-$  anions, respectively. The latter shows the best  $OCS^-$  signal that could be achieved in the experiment. The ion peaks in (a) and (b) labeled in accordance with the corresponding anion mass (in a.m.u.) are assigned as follows:  $66 = {}^{32}S\,{}^{34}S^-$ ;  $76 = CS_2^-$ ;  $80 = OC^{34}S^- \cdot H_2O$ ;  $82 = S_2^- \cdot H_2O$ ;  $92 = OCS_2^-$ ;  $124 = S_2^- \cdot OCS$ ;  $132 = OCS^- \cdot (H_2O)_4$ ;  $150 = OCS^- \cdot (H_2O)_5$ . In (c), the top of the three combs above the mass spectrum indicates the peak positions for the  $(OCS)_n^-$  cluster anions ( $n = 4 - 10$ ). The two lower combs correspond to the monohydrated  $(OCS)_n^- \cdot H_2O$  and doubly hydrated  $(OCS)_n^- \cdot (H_2O)_2$  cluster ions, respectively.

ticularly on the position of the 1 keV electron beam relative to the nozzle. The magnified spectrum in Fig. 1(b) was recorded under the conditions optimized for the formation of  $OCS^-$  and represents the best  $OCS^-$  signal that could be achieved. In most cases, without special efforts to optimize this signal, no  $OCS^-$  could be discerned at all, while other ion peaks remained robust.

On the other hand, there is an intense progression of peaks corresponding to  $[OCS(H_2O)_k]^-$  with  $k$  from 1 to at least 5. In Figs. 1(a) and 1(b), the peaks corresponding to  $OCS^-$  hydrated by one, two, and three water molecules are labeled explicitly, while peaks 132 and 150 correspond to  $OCS^- \cdot (H_2O)_4$  and  $OCS^- \cdot (H_2O)_5$ , respectively. Careful examination of the spectrum reveals that all  $OCS^- \cdot (H_2O)_k$  ion peaks are followed by satellite isotope peaks with relative intensities characteristic of anions containing one sulfur atom.

Since one water molecule does not bind an electron,<sup>61–69</sup>

the  $k = 1$  cluster is described as  $OCS^- \cdot H_2O$ . For  $k > 1$ , the question of electron localization is open, but by analogy with  $CO_2^- \cdot (H_2O)_k$ ,<sup>11,70–72</sup> it is reasonable to assume that the electron is localized on the  $OCS^-$  cluster core. In view of the insignificant  $OCS^-$  signal, the efficient formation of the  $OCS^- \cdot (H_2O)_k$  cluster ions is quite revealing. In particular, it is remarkable that the  $OCS^- \cdot H_2O$  peak is one of the most intense peaks in the spectrum, while the seemingly simpler  $OCS^-$  anion is barely observed at all.

Another intense peak in Fig. 1(b), followed by a series of satellite peaks characteristic of a compound with two sulfur atoms, corresponds to the  $(OCS)_2^-$  anion. Lineberger and co-workers argued that it is not an  $OCS^- \cdot OCS$  cluster, but a covalently bound dimer anion, whose structure has little in common with the  $OCS^-$  monomer.<sup>9</sup> Therefore, the  $(OCS)_2^-$  anion sheds little light on the structure of hydrated  $OCS^- \cdot (H_2O)_k$  anions. However, the question of whether the  $(OCS)_2^- \cdot (H_2O)_k$  cluster ions possess monomer or dimer anion cores is open.

Figure 1(c) shows a mass spectrum optimized for heavier cluster ions. The sharp onset of the signal in the vicinity of 200 a.m.u. is due to the truncation of the spectrum by the potential switch. The spectrum has prominent progressions of peaks corresponding to  $[(OCS)_n(H_2O)_k]^-$  with  $n = 3 - 10$  and  $k = 0 - 2$ . The cluster ions with  $k > 2$  are most likely present as well, but remain unresolved due to the overlap with other peaks.

The structure of  $[(OCS)_n(H_2O)_k]^-$  ( $n \geq 2, k \geq 1$ ) cluster ions is not obvious and will be tested in the future by photoelectron imaging spectroscopy. For  $k \geq 2$  and particularly for larger  $k$ , hydration of the electron cannot be ruled out. Although we tentatively describe these clusters as hydrated anions of OCS, some may correspond to  $(H_2O)_k^-$ , additionally solvated by OCS molecules. It is possible that these clusters preserve the dimer core structure of unhydrated  $(OCS)_n^-$ , predicted for  $n < 16$ ,<sup>9</sup> but we also cannot discount the possibility that the solvation energetics in  $(OCS)_n^- \cdot (H_2O)_k$  shift in favor of the  $OCS^-$  monomer cluster core.

To summarize the experimental results, the  $OCS^-$  anions are formed extremely inefficiently in an electron-impact ionized OCS–Ar expansion. Nonetheless, the hydrated cluster anions, including in particular  $OCS^- \cdot H_2O$ , are produced readily and in abundance, as well as the larger  $[(OCS)_n(H_2O)_k]^-$  cluster ions. In the next Section, we combine these observations with theoretical evidence that OCS has no electron affinity and discuss the stabilization of metastable  $OCS^-$  by gas phase hydration, as the effect responsible for the stability of the  $OCS^- \cdot (H_2O)_k$  clusters.

## IV. THEORETICAL RESULTS AND DISCUSSION

### A. Adiabatic electron affinity of OCS

The definition of adiabatic EA as the energy difference between the lowest-energy states of the neutral and the anion becomes ambiguous if the calculated EA turns out negative. A negative EA implies that the relaxed neutral species lies lower in energy than the corresponding anion (e.g.,  $CO_2$  vs  $CO_2^-$ ). However, it immediately follows that in such a case

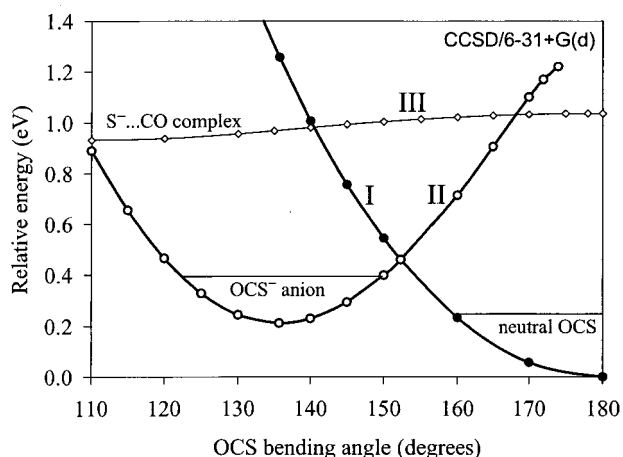


FIG. 2. The relaxed diabatic potential energy curves of OCS (curve I: filled circles),  $\text{OCS}^-$  (curve II: open circles, bold line), and  $\text{S}^- \cdots \text{CO}$  (curve III: open symbols, thin line), calculated along the bending coordinate at the CCSD theory level with the 6-31+G(d) basis set. Curve I also corresponds to the  $\text{OCS} + e^-$  detached-electron state. In the  $\text{S}^- \cdots \text{CO}$  anion-neutral complex (curve III), the typical C-S distance is in the 3.2–3.7 Å range. The horizontal lines above the OCS and  $\text{OCS}^-$  potential minima indicate the ground state energies corrected for the ZPE.

the most stable anionic state is a relaxed neutral molecule plus a free electron ( $e^-$ ), and therefore, the truly adiabatic EA is not negative, but zero, or—it is said—nonexistent. Accordingly, a calculation within the Born–Oppenheimer limit sampling the entire coordinate space and employing a sufficiently large basis set must yield an EA approaching zero. Unfortunately, this conclusion tells little about the structure of the metastable anion of interest. It does show, however, that it is important to clarify what is meant by reporting negative values of adiabatic EA.

We begin our investigation of the EA of OCS by exploring the OCS and  $\text{OCS}^-$  bending potentials with relatively inexpensive calculations. Figure 2 shows portions of the OCS and  $\text{OCS}^-$  potential energy curves calculated along the bending coordinate using the CCSD theory with the 6-31+G(d) basis set. For each OCS angle, the CO and CS bondlengths in both the neutral and the anion were optimized to yield the relaxed potential energy curves. The three curves in Fig. 2 correspond to the following diabatic states: (I) the neutral OCS molecule or the  $\text{OCS} + e^-$  (detached-electron) state; (II) the  $\text{OCS}^-$  molecular anion; and (III) the  $\text{S}^- \cdots \text{CO}$  anion-neutral complex (corresponding to C–S distances of 3.2–3.7 Å). The horizontal lines above the OCS and  $\text{OCS}^-$  potential minima indicate the ground-state energies corrected for the zero-point vibrational energy (ZPE). The relaxed OCS has lower energy than  $\text{OCS}^-$ , indicating that the EA, defined as the difference between the two potential minima, is negative.

The crossing between curves I and II, corresponding to the diabatic  $\text{OCS} + e^-$  and  $\text{OCS}^-$  states, defines the adiabatic ground state of the anionic system, which has an electron-bound ( $\text{OCS}^-$ ) and free-electron characters to the left and to the right of the I/II crossing point in Fig. 2, respectively. There is a potential barrier on the adiabatic bending potential, separating the bent  $\text{OCS}^-$  equilibrium from the more

energetically favorable linear  $\text{OCS} + e^-$  system. If  $\text{OCS}^-$  is formed within the potential well corresponding to the electron-bound state, it is isolated from the part of the potential energy surface where the autodetachment would occur. The barrier separating the  $\text{OCS}^-$  and  $\text{OCS} + e^-$  equilibria is estimated to be higher than the I/II intersection point at  $\angle\text{OCS} = 152.3^\circ$  in Fig. 2, because this point in fact corresponds to two different geometries of the neutral and the anion ( $R_{\text{CO}} = 1.171$  Å,  $R_{\text{CS}} = 1.587$  Å for the neutral;  $R_{\text{CO}} = 1.216$  Å,  $R_{\text{CS}} = 1.685$  Å for the anion). The metastable  $\text{OCS}^-$  state may explain the observation of minor quantities of  $\text{OCS}^-$  in the present experiment, as well as the  $\text{OCS}^-$  fragments in the  $(\text{OCS})_2^-$  photodissociation, which were found to be stable on a  $>5$   $\mu\text{s}$  time scale.<sup>9</sup>

Defining the EA as the energy difference between the neutral state and the electron-bound  $\text{OCS}^-$  state, the EA of OCS was calculated at several *ab initio* and DFT theory levels, employing a variety of basis sets. Except where single-point calculations are indicated, the geometries of OCS and  $\text{OCS}^-$  were optimized at the indicated theory level. The results of the *ab initio* and composite theory calculations are summarized in Table I. The EA values determined by Gutsev *et al.*<sup>28</sup> are also included. For comparison, Table II lists the EAs determined by several DFT methods.

The optimized geometries and vibrational frequencies determined at selected theory levels are given in Table III, along with the zero-point vibrational energies and  $\Delta\text{ZPE}$  corrections to the EA ( $\Delta\text{ZPE}$  is defined as the difference between the ZPEs of OCS and  $\text{OCS}^-$ ). The EA of OCS, corrected for the ZPEs, is obtained by adding  $\Delta\text{ZPE}$  to the purely electronic EA values listed in Tables I and II. While  $\Delta\text{ZPE}$  varies slightly with the theory level and basis set, the rounded-off correction  $\Delta\text{ZPE} = 0.07$  eV, consistent with most calculations, is sufficient for this discussion.

Some of the results for the EA, including the  $\Delta\text{ZPE}$  correction, are summarized in a graphic form in Fig. 3. Our strategy in selecting data for this plot has been to choose the results obtained with the largest basis set for each type of calculations. The *ab initio* results are arranged in the general order of increasing the level of electron correlation. All *ab initio* methods predict that the adiabatic EA is either negative or essentially zero. The largest in magnitude negative values of EA are predicted by MP2. While almost always remaining negative, the absolute magnitude of the EA tends to decrease, approaching zero, as the correlation effects beyond the second-order perturbation theory are included. The basis sets of Dunning (open circles in Fig. 3) tend to yield higher (less negative) EA values than the basis sets of Pople (filled circles).

Special consideration is given to the G3 theory value of  $\text{EA} = -0.059$  eV. Not surprisingly, the largest correction for the EA within the G3 calculation comes from the inclusion of diffuse basis functions, underscoring their importance for proper modeling of the electronic structure of  $\text{OCS}^-$ . The total energy correction for diffuse functions  $\Delta E(+)$  is  $-0.03099$  hartrees for the anion compared to  $-0.00840$  hartrees for the neutral, increasing the calculated EA by 0.615 eV.

The known test statistics for the G2 and G3 theories are

TABLE I. Calculated values of the electron affinity of OCS, excluding the zero-point vibrational energy corrections ( $\Delta ZPE$ ), except where noted.

Method	Basis set	EA, eV (excluding $\Delta ZPE$ )
<b>HF</b>	6-31+G( <i>d</i> )	<b>-0.209</b>
	6-311+G(3 <i>df</i> )	<b>-0.394<sup>a</sup></b>
<b>MP2</b>	6-31+G( <i>d</i> )	<b>-0.510</b>
	aug-cc-pVDZ	<b>-0.315<sup>b</sup></b>
	aug-cc-pVTZ	<b>-0.335<sup>b</sup></b>
<b>MP2 (full)</b>	aug-cc-pVDZ	<b>-0.338<sup>b</sup></b>
<b>MP3 (full)</b>	aug-cc-pVDZ	<b>-0.100<sup>b</sup></b>
<b>MP4-SDTQ</b>	6-31+G( <i>d</i> )	<b>-0.459<sup>b</sup></b>
<b>MP4-SDTQ (full)</b>	aug-cc-pVDZ	<b>-0.239<sup>b</sup></b>
<b>CCSD</b>	6-31+G( <i>d</i> )	<b>-0.211</b>
	6-311+G( <i>d</i> )	<b>-0.284</b>
	6-311+G(2 <i>df</i> )	<b>-0.203</b>
	aug-cc-pVDZ	<b>-0.035</b>
	aug-cc-pVTZ	<b>-0.059<sup>c</sup></b>
<b>CCSD (full)</b>	6-31+G( <i>d</i> )	<b>-0.237</b>
	6-311+G( <i>d</i> )	<b>-0.295</b>
	aug-cc-pVDZ	<b>-0.058</b>
<b>CCSD(T)</b>	6-311+G( <i>d</i> )	<b>-0.342</b>
	6-311+G(3 <i>df</i> )	<b>-0.295<sup>a</sup></b>
	aug-cc-pVDZ	<b>-0.071</b>
<b>CCSD(T)</b>	G3large	
<b>MP2</b>		-0.439
<b>MP3</b>		-0.217
<b>MP4-SDTQ</b>		-0.336
<b>CCSD</b>		-0.162
<b>CCSD(T)</b>		<b>-0.190</b>
<b>QCISD(T)</b>	6-31+G( <i>d</i> )	<b>-0.276</b>
	6-311+G( <i>d</i> )	<b>-0.342</b>
	aug-cc-pVDZ	<b>-0.067</b>
<b>Composite theories (incl. ZPE):</b>		
Gaussian-1 (G1)		<b>-0.107<sup>d</sup></b>
Gaussian-2 (G2)		<b>-0.095<sup>d</sup></b>
Gaussian-3 (G3)		<b>-0.059<sup>d</sup></b>

<sup>a</sup>From Gutsev *et al.* (Ref. 28).<sup>b</sup>From single-point calculations at the geometries optimized at the MP2/6-31+G(*d*) level.<sup>c</sup>From single-point calculations at the geometries optimized at the CCSD/aug-cc-pVDZ level.<sup>d</sup>Includes the  $\Delta ZPE$  correction.

used here to arrive at meaningful trust margins for the calculated values of EA. The average absolute deviation of the G3 electron affinities from the experimental data has been determined to be 1.00 kcal/mol, or 43 meV, compared to 1.41 kcal/mol, or 61 meV for the predecessor G2 theory.<sup>37</sup> More importantly, 62% of the EAs calculated using the G3 method fall within 1.0 kcal/mol of the experimental values for the G2/97 test set species, while 76% fall within 1.4 kcal/mol (61 meV).<sup>37</sup> For G2, similar measures are: 55% within 1.4 kcal/mol of the experiment and 76% within 2.0 kcal/mol (87 meV).<sup>37</sup> Based on these assessments, we assign the following margins of trust (with estimated 76% confidence) for the EA of OCS calculated here using the G3 and G2 theories: EA =  $-0.059 \pm 0.061$  eV for G3 and  $-0.095 \pm 0.087$  eV for G2.

Contrary to the *ab initio* methods, the DFT calculations with moderate-size basis sets yield positive values of the adiabatic EA of OCS. However, the calculated EA decreases consistently as the size of the basis set is increased. For example, the *mPW1PW91* method employed with Dunning's basis sets predicts the values of EA that reverse sign

TABLE II. Calculated DFT values of the electron affinity of OCS, excluding the zero-point vibrational energy corrections ( $\Delta ZPE$ ).

Method	Basis set	EA, eV (excluding $\Delta ZPE$ )
<b>BLYP</b>	6-31+G( <i>d</i> )	0.065
	6-311+G( <i>d</i> )	0.021
	aug-cc-pVDZ	0.074
	aug-cc-pVTZ	-0.020
	aug-cc-pVQZ	-0.033
<b>B3LYP</b>	6-31+G( <i>d</i> )	0.226
	6-311+G( <i>d</i> )	0.164
	6-311+G(3 <i>df</i> )	0.059
	G3large	0.061
	aug-cc-pVDZ	0.208
<b>mPW1PW91</b>	aug-cc-pVTZ	0.103
	aug-cc-pVQZ	0.085
	6-31+G( <i>d</i> )	0.170
	6-311+G( <i>d</i> )	0.104
	6-311+G(3 <i>df</i> )	-0.003
	aug-cc-pVDZ	0.149
	aug-cc-pVTZ	0.041
	aug-cc-pVQZ	-0.147

from positive to negative as the basis set is expanded from double to quadruple- $\zeta$  (see Table II).

Tschumper and Schaefer estimated average absolute errors of 0.25 and 0.18 eV for the EAs of triatomics predicted using the B3LYP and BLYP methods, respectively.<sup>54</sup> Scaling these average values by a factor of 1.4, for a higher confidence level similar to the above G3 and G2 analyses, we arrive at the following margins of trust for some of our DFT results (including the  $\Delta ZPE$  corrections): EA =  $0.13 \pm 0.35$  eV for the B3LYP calculations with both the 6-311+G(3*df*) and G3large basis sets and  $0.09 \pm 0.25$  eV for the BLYP/6-311+G(*d*) result.

The margins of trust for the G2, G3, BLYP, and B3LYP calculations are indicated as error bars in Fig. 3. Given the large margins estimated for DFT, there is no discrepancy between the G3 and G2 predictions on the one hand, and the DFT results on the other. The G3 and G2 values are also consistent with most coupled-cluster and quadruple CI theory results. We thus conclude that the EA of OCS is either slightly negative or zero. In the strict adiabatic sense, our overall conclusion is that OCS has no electron affinity.

This conclusion is in disagreement with the 1975 collisional detachment measurement, which placed the EA of OCS at  $0.46 \pm 0.2$  eV.<sup>10</sup> However, the preponderance of theoretical evidence, corroborated by the indirect experimental observations, indicates that the EA cannot be substantially positive. Even so, the metastable OCS<sup>-</sup> anions can be formed via a dynamic process involving a favorable (bent) geometry, as in the case of (OCS)<sub>2</sub><sup>-</sup> dissociation, where the parent dimer anion has two covalently joined, bent OCS moieties.<sup>9</sup>

## B. Structure and energetics of OCS<sup>-</sup>·H<sub>2</sub>O

Given the nonexistent EA of OCS, the corresponding anions exist in the stable, hydrated form due to the additional stabilization resulting from the strong ion-neutral interac-

TABLE III. Calculated equilibrium geometries and vibrational frequencies of OCS and OCS<sup>-</sup>.

	HF 6-31G( <i>d</i> )	CCSD 6-31+G( <i>d</i> )	CCSD 6-311+G( <i>d</i> )	CCSD(T) G3large	B3LYP G3large
Neutral OCS <sup>a</sup>					
<i>R</i> <sub>CO</sub> , Å	1.1314	1.1670	1.1557	1.1598	1.1555
<i>R</i> <sub>CS</sub> , Å	1.5723	1.5703	1.5683	1.5675	1.5616
<i>ω</i> <sub>1</sub> , cm <sup>-1</sup>	794 <sup>b</sup>	884	888		880
<i>ω</i> <sub>2</sub> , cm <sup>-1</sup>	506 <sup>b</sup>	493	505		530
<i>ω</i> <sub>3</sub> , cm <sup>-1</sup>	2059 <sup>b</sup>	2118	2137		2112
ZPE, eV	0.2396 <sup>b</sup>	0.2472	0.2501		0.2512
OCS <sup>-</sup> Anion					
<i>R</i> <sub>CO</sub> , Å	1.1869	1.2175	1.2074	1.2103	1.2058
<i>R</i> <sub>CS</sub> , Å	1.7318	1.7116	1.7103	1.7067	1.7013
∠OCS, °	135.12	135.69	135.69	136.69	136.98
<i>ω</i> <sub>1</sub> , cm <sup>-1</sup>	676 <sup>b</sup>	740	735		703
<i>ω</i> <sub>2</sub> , cm <sup>-1</sup>	463 <sup>b</sup>	498	500		487
<i>ω</i> <sub>3</sub> , cm <sup>-1</sup>	1717 <sup>b</sup>	1712	1718		1684
ZPE, eV	0.1771 <sup>b</sup>	0.1829	0.1831		0.1782
ΔZPE, eV	0.063 <sup>b</sup>	0.064	0.067		0.073

<sup>a</sup>The experimental values for OCS are: *R*<sub>CO</sub>=1.1562 Å, *R*<sub>CS</sub>=1.5614 Å, and vibrational frequencies 875.3, 524.4, and 2093.7 cm<sup>-1</sup> (Ref. 76).

<sup>b</sup>The HF/6-31G(*d*) frequencies and ZPEs are scaled by a factor of 0.8929. Others are unscaled.

tions between OCS<sup>-</sup> and H<sub>2</sub>O. The experiment indicates that the addition of one water molecule is sufficient to offset the negative value of the EA. This is not surprising, considering the small absolute values of the negative EA predicted above.

We determined theoretically the structures of four OCS<sup>-</sup>·H<sub>2</sub>O isomers, which are shown in Fig. 4. The four structures were first obtained from a B3LYP/6-311++G(*d,p*) geometry optimization (the corresponding struc-

tural and energetic parameters are given in italics in Fig. 4) and then re-optimized at the CCSD level with the 6-31+G(*d*) basis set (plain font in Fig. 4). In addition, the most stable structure [Fig. 4(A)] was optimized at the CCSD level with the 6-311++G(*d,p*) basis set (bold in Fig. 4) and the *m*PW1PW91 DFT level with the aug-cc-pVTZ basis (italics in parentheses in Fig. 4). Only the most important intermolecular parameters are given in Fig. 4, while Table IV lists the complete set of parameters and the harmonic vibrational frequencies of the ground-state structure [Fig. 4(A)], as determined from the CCSD/6-311++G(*d,p*) calculation.

All structures are characterized by the excess electron localized on OCS and all four have planar equilibrium geometries. They correspond to true potential minima, as verified by their real harmonic vibrational frequencies. Care was taken to determine all possible structural isomers by starting the optimization from different initial configurations. The initial intermolecular coordinates for the optimizations were chosen to be analogous to the three isomers predicted for CO<sub>2</sub><sup>-</sup>·H<sub>2</sub>O, which are: One of the *C*<sub>2v</sub> symmetry with two equivalent electrostatic O–H “bonds” and two *C*<sub>s</sub> structure-with single O–H “bonds,” one each in the *cis* and *trans* configurations of the dangling H atom with respect to CO<sub>2</sub><sup>-</sup>.<sup>11,73</sup> Considering the reduced symmetry of OCS<sup>-</sup>, five different structures might be expected for OCS<sup>-</sup>·H<sub>2</sub>O: An isomer with the electrostatic O–H and S–H bonds, in addition to two *trans* and two *cis* structures with dangling hydrogen atoms, one each on the oxygen and sulfur sides of OCS<sup>-</sup>. However, one of the sulfur-side structures proved to be a saddle point on the potential leading to the global minimum [Fig. 4(A)], and thus only four isomers corresponding to true potential minima were found.

The important energetic parameter describing the relative stability of the cluster is the hydration energy Δ*E*<sub>*h*</sub>, defined here as the electronic energy (excluding the ZPE) of OCS<sup>-</sup>·H<sub>2</sub>O relative to the separated OCS<sup>-</sup>+H<sub>2</sub>O limit. The calculated values of Δ*E*<sub>*h*</sub> are indicated in Fig. 4, along with

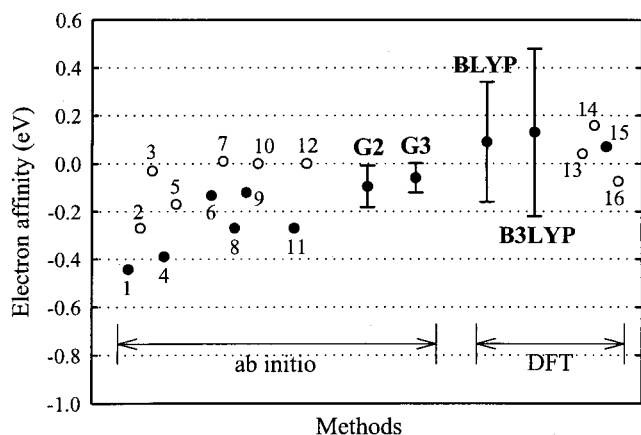


FIG. 3. Some of the results for the adiabatic EA of OCS, including the ΔZPE correction. Open and filled circles: Results obtained with the augmented correlation consistent basis sets of Dunning and the split valence basis sets of Pople, respectively. The error bars for the G2, G3, BLYP, and B3LYP results are determined as described in the text. The BLYP result was obtained with the 6-311+G(*d*) basis set, while both the 6-311+G(3*df*) and G3large basis sets yielded the B3LYP value shown. Other data points are as follows: 1—MP2/6-31+G(*d*); 2—MP2/aug-cc-pVTZ; 3—MP3(Full)/aug-cc-pVDZ; 4—MP4(Full)/6-31+G(*d*); 5—MP4(Full)/aug-cc-pVDZ; 6—CCSD/6-311+G(2*df*); 7—CCSD/aug-cc-pVTZ; 8—CCSD(T)/6-311+G(*d*); 9—CCSD(T)/G3large; 10—CCSD(T)/aug-cc-pVDZ; 11—QCISD(T)/6-311+G(*d*); 12—QCISD(T)/aug-cc-pVDZ; 13—BLYP/aug-cc-pVQZ; 14—B3LYP/aug-cc-pVQZ; 15—*m*PW1PW91/6-31+G(3*df*); 16—*m*PW1PW91/aug-cc-pVQZ.

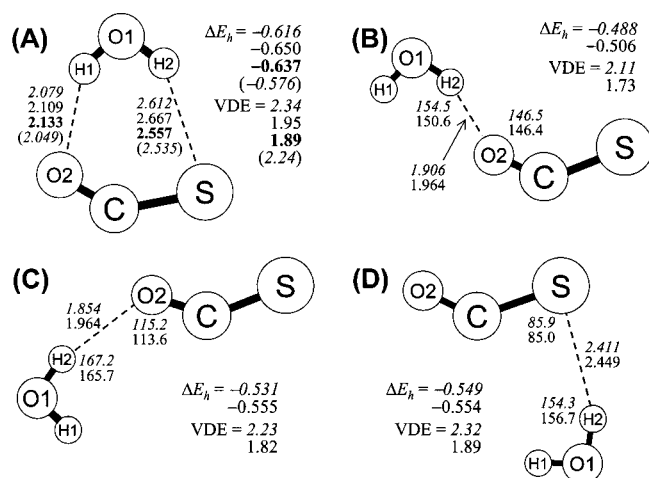


FIG. 4. The equilibrium structures of four  $\text{OCS}^- \cdot \text{H}_2\text{O}$  isomers. The relative hydration energies  $\Delta E_h$  and VDEs are given in eV, while the intermolecular structural parameters are in Angstroms and degrees. The indicated values of  $\Delta E_h$  are the purely electronic (excluding the ZPE correction) hydration energies, defined as the energy of  $\text{OCS}^- \cdot \text{H}_2\text{O}$  relative to the sum of the separated  $\text{OCS}^-$  and  $\text{H}_2\text{O}$  energies. The energetic and structural parameters are determined from the following calculations: listed first (italics)—B3LYP/6-311++G(*d,p*); listed second (plain font)—CCSD/6-31+G(*d*). For the lowest-energy structure (A), the parameters listed third (bold) are from CCSD/6-311++G(*d,p*), and those listed last (italics in parentheses) are at the *mPW1PW91/aug-cc-pVTZ* level.

the predicted vertical detachment energies (VDE) for each isomer. In particular, for the most stable isomer (structure A),  $\Delta E_h = -0.637$  eV at the CCSD/6-311++G(*d,p*) level. The corresponding  $\Delta ZPE$  correction, found using the frequencies in Table IV, is 0.094 eV, and thus structure A is stabilized by 0.543 eV relative to the separated  $\text{OCS}^- + \text{H}_2\text{O}$  limit. This value is in line with the typical stabilization expected for an ion-dipole interaction ( $\sim 0.6$  eV)<sup>74,75</sup> and similar to the stabilization energy observed for  $\text{CO}_2^-$  hydrates.<sup>11</sup>

### C. Comparison of the hydrated anions of $\text{CO}_2$ , $\text{OCS}$ , and $\text{CS}_2$

These results allow for a comparison of the hydration of the isovalent  $\text{CO}_2^-$ ,  $\text{OCS}^-$ , and  $\text{CS}_2^-$  anions, with  $\text{OCS}^-$  bridging the gap between the other two.

For  $\text{CO}_2$  (EA =  $-0.6$  eV),<sup>10</sup> the unhydrated anion is metastable, and it takes at least two  $\text{H}_2\text{O}$  molecules for the efficient formation of hydrated  $\text{CO}_2^-$  in an electron-impact source, i.e., the smallest hydrated cluster anion formed in abundance under conditions similar to ours is  $\text{CO}_2^- (\text{H}_2\text{O})_2$ .<sup>11,70</sup> In Sec. III, we showed that the corresponding minimum number of water molecules in the hydration of  $\text{OCS}^-$  is reduced to one. Finally, the  $\text{CS}_2^-$  anion requires no external stabilization, as the EA of  $\text{CS}_2$  is in the 0.9–1.0 eV range.<sup>10,27</sup>

Another parallel can be drawn for the hydration of the corresponding dimer anions, where a similar trend of the diminishing required hydration is observed. Indeed, although

TABLE IV. Equilibrium parameters and unscaled harmonic vibrational frequencies of  $\text{OCS}^- \cdot \text{H}_2\text{O}$  (ground-state structure A shown in Fig. 4) calculated at the CCSD level with the 6-311++G(*d,p*) basis set.

Structural parameters (Å and degrees)		Vibrational modes and harmonic frequencies		
		Symmetry	Approximate description of the mode dominant character	$\text{cm}^{-1}$
C–O2	1.211	$a'$		102
C–S	1.707	$a''$		107
O2–C–S	135.5	$a'$		159
S–H2	2.557	$a''$	H <sub>2</sub> O twisting out of plane (H atoms moving up/down in opposite directions)	328
H2–S–C	84.0	$a'$	In-plane rocking motion of H <sub>2</sub> O relative to OCS <sup>-</sup>	338
O1–H2	0.966	$a'$		512
O1–H1–H2	99.1	$a'$	OCS <sup>-</sup> bending <sup>a</sup>	512
O1–H2–S	146.6	$a''$	H <sub>2</sub> O tilting out of plane (both H moving synchronously up or down)	618
O2–H1	2.133	$a'$	CS stretch <sup>b</sup>	748
		$a'$	CO stretch <sup>c</sup>	1700
		$a'$	H <sub>2</sub> O bending <sup>d</sup>	1745
		$a'$	H <sub>2</sub> O symmetric stretch <sup>e</sup>	3802
		$a'$	H <sub>2</sub> O antisymmetric stretch <sup>f</sup>	3860

<sup>a</sup>For comparison, the CCSD/6-311+G(*d*) bending frequency in free  $\text{OCS}^-$  is  $500 \text{ cm}^{-1}$  (all frequencies are unscaled).

<sup>b</sup>The corresponding frequency in free  $\text{OCS}^-$  is  $735 \text{ cm}^{-1}$ .

<sup>c</sup>The corresponding frequency in free  $\text{OCS}^-$  is  $1718 \text{ cm}^{-1}$ .

<sup>d</sup>The CCSD/6-311++G(*d,p*) bending frequency in free  $\text{H}_2\text{O}$  is  $1656 \text{ cm}^{-1}$ .

<sup>e</sup>The CCSD/6-311++G(*d,p*) symmetric stretch frequency in free  $\text{H}_2\text{O}$  is  $3896 \text{ cm}^{-1}$ .

<sup>f</sup>The CCSD/6-311++G(*d,p*) antisymmetric stretch frequency in free  $\text{H}_2\text{O}$  is  $3997 \text{ cm}^{-1}$ .

$(\text{CO}_2)_2^-$  can be formed,<sup>3,4,14</sup> its abundance is small compared to the  $(\text{CO}_2)_2^- \cdot \text{H}_2\text{O}$  cluster anion.<sup>11</sup> Thus, one water molecule is needed to stabilize effectively  $(\text{CO}_2)_2^-$ , while  $(\text{OCS})_2^-$  and  $(\text{CS}_2)_2^-$  are both stable and abundant in the isolated form.<sup>2,9</sup> These observations can be summarized in an empirical 3-2-1 rule: For the efficient formation of stable  $X_n^-(\text{H}_2\text{O})_k$  cluster ions ( $X = \text{CO}_2$ ,  $\text{OCS}$ , or  $\text{CS}_2$ ) with  $n \geq 1$ , the total number of molecules ( $n+k$ ) must be at least 3, 2, and 1, respectively.

## V. SUMMARY AND FUTURE DIRECTIONS

In summary, we observed the efficient formation of the  $[(\text{OCS})_n(\text{H}_2\text{O})_k]^-$  ( $n \geq 1, n+k \geq 2$ ) cluster ions, of which  $\text{OCS}^- \cdot \text{H}_2\text{O}$  is the most interesting species in view of the near absence of the seemingly simpler  $\text{OCS}^-$  in the same ion source. The presence of the monohydrated anion is attributed to the stabilization of  $\text{OCS}^-$  by hydration and serves as unambiguous proof that the intra-cluster formation of  $\text{OCS}^-$  monomers is a part of the  $[(\text{OCS})_n(\text{H}_2\text{O})_k]^-$  dynamics. In this light, the inefficient formation of unhydrated  $\text{OCS}^-$  is attributed to the nonexistent adiabatic electron affinity of  $\text{OCS}$ , as indicated by theoretical calculations. The photoelectron imaging experiments, currently in progress in our laboratory, will provide insights into the energetics and electronic structure of the hydrated anions of  $\text{OCS}$ .

## ACKNOWLEDGMENTS

The authors would like to thank W. Carl Lineberger and Hanna Reisler for invaluable advice on building the experimental apparatus and establishing the research program. We are particularly thankful to Professor Lineberger for provoking our interest in carbonyl sulfide anions, which dates back to the experiment on  $(\text{OCS})_n^-$  carried out in the Lineberger laboratory, where A.S. was a postdoctoral fellow.<sup>9</sup> We are grateful to Kenneth D. Jordan and Ludwik Adamowicz for the discussions of the theoretical aspects of the project, and thank Ludwik Adamowicz for his comments on Sec. IV of the manuscript. We also wish to thank Stephen G. Kukolich for sharing the design of the pulsed valve driver circuit. This work is supported in part by the ACS Petroleum Research Fund (ACS-PRF Grant No. 35589-G6) and the Research Corporation (Research Innovation Award No. RI0515).

- <sup>1</sup>A. W. Castleman and K. H. Bowen, *J. Phys. Chem.* **100**, 12911 (1996).
- <sup>2</sup>T. Maeyama, T. Oikawa, T. Tsumura, and N. Mikami, *J. Chem. Phys.* **108**, 1368 (1998).
- <sup>3</sup>M. J. DeLuca, B. Niu, and M. A. Johnson, *J. Chem. Phys.* **88**, 5857 (1988).
- <sup>4</sup>T. Tsukuda, M. A. Johnson, and T. Nagata, *Chem. Phys. Lett.* **268**, 429 (1997).
- <sup>5</sup>T. Tsukuda, T. Hirose, and T. Nagata, *Chem. Phys. Lett.* **279**, 179 (1997).
- <sup>6</sup>K. H. Bowen and J. G. Eaton, in *The Structure of Small Molecules and Ions*, edited by R. Naaman and Z. Vager (Plenum, New York, 1988), p. 147.
- <sup>7</sup>K. Hiraoka, S. Fujimaki, G. Aruga, and S. Yamabe, *J. Phys. Chem.* **98**, 1802 (1994).
- <sup>8</sup>S. H. Fleischman and K. D. Jordan, *J. Phys. Chem.* **91**, 1300 (1987).
- <sup>9</sup>A. Sanov, S. Nandi, K. D. Jordan, and W. C. Lineberger, *J. Chem. Phys.* **109**, 1264 (1998).
- <sup>10</sup>R. N. Compton, P. W. Reinhardt, and C. D. Cooper, *J. Chem. Phys.* **63**, 3821 (1975).

- <sup>11</sup>T. Tsukuda, M. Saeki, R. Kimura, and T. Nagata, *J. Chem. Phys.* **110**, 7846 (1999).
- <sup>12</sup>C. D. Cooper and R. N. Compton, *Chem. Phys. Lipids* **14**, 29 (1972).
- <sup>13</sup>C. D. Cooper and R. N. Compton, *J. Chem. Phys.* **59**, 3550 (1973).
- <sup>14</sup>C. E. Klots and R. N. Compton, *J. Chem. Phys.* **67**, 1779 (1977).
- <sup>15</sup>C. E. Klots and R. N. Compton, *J. Chem. Phys.* **69**, 1636 (1978).
- <sup>16</sup>M. L. Alexander, M. A. Johnson, N. E. Levinger, and W. C. Lineberger, *Phys. Rev. Lett.* **57**, 976 (1986).
- <sup>17</sup>M. L. Alexander, Ph.D., University of Colorado, 1987.
- <sup>18</sup>M. Knapp, D. Kreisle, O. Echt, K. Sattler, and E. Recknagel, *Surf. Sci.* **156**, 313 (1985).
- <sup>19</sup>M. Knapp, O. Echt, D. Kreisle, T. D. Mark, and E. Recknagel, *Chem. Phys. Lett.* **126**, 225 (1986).
- <sup>20</sup>A. Stamatovic, K. Leiter, W. Ritter, K. Stephan, and T. D. Mark, *J. Chem. Phys.* **83**, 2942 (1985).
- <sup>21</sup>H. Langosh and H. Haberland, *Z. Phys. D: At., Mol. Clusters* **2**, 243 (1986).
- <sup>22</sup>T. Kondow and K. Mitsuke, *J. Chem. Phys.* **83**, 2612 (1985).
- <sup>23</sup>T. Kondow, *J. Phys. Chem.* **91**, 1307 (1987).
- <sup>24</sup>F. Misaizu, K. Mitsuke, T. Kondow, and K. Kuchitsu, *J. Chem. Phys.* **94**, 243 (1991).
- <sup>25</sup>T. Kraft, M. W. Ruf, and H. Hotop, *Z. Phys. D: At., Mol. Clusters* **14**, 179 (1989).
- <sup>26</sup>A. Sanov, W. C. Lineberger, and K. D. Jordan, *J. Phys. Chem. A* **102**, 2509 (1998).
- <sup>27</sup>J. M. Oakes and G. B. Ellison, *Tetrahedron* **42**, 6263 (1986).
- <sup>28</sup>G. L. Gutsev, R. J. Bartlett, and R. N. Compton, *J. Chem. Phys.* **108**, 6756 (1998).
- <sup>29</sup>*CRC Handbook of Chemistry and Physics*, 81 ed. (CRC Press, Boca Raton, FL, 2000).
- <sup>30</sup>C. E. Klots, *J. Chem. Phys.* **83**, 5854 (1985).
- <sup>31</sup>M. A. Johnson and W. C. Lineberger, in *Techniques for the Study of Ion Molecule Reactions*, edited by J. M. Farrar and J. W. Saunders (Wiley, New York, 1988), p. 591.
- <sup>32</sup>M. E. Nadal, P. D. Kleiber, and W. C. Lineberger, *J. Chem. Phys.* **105**, 504 (1996).
- <sup>33</sup>S. G. Kukolich (private communication).
- <sup>34</sup>W. C. Wiley and I. H. McLaren, *Rev. Sci. Instrum.* **26**, 1150 (1955).
- <sup>35</sup>L. A. Posey, M. J. Deluca, and M. A. Johnson, *Chem. Phys. Lett.* **131**, 170 (1986).
- <sup>36</sup>M. J. Frisch, G. W. Trucks, H. B. Schlegel *et al.*, GAUSSIAN 98, Rev. A.7 Gaussian, Inc., Pittsburgh, PA, 1998.
- <sup>37</sup>L. A. Curtiss, K. Raghavachari, P. C. Redfern, V. Rassolov, and J. A. Pople, *J. Chem. Phys.* **109**, 7764 (1998).
- <sup>38</sup>C. Møller and M. S. P. R. Plesset, *Phys. Rev.* **46**, 618 (1934).
- <sup>39</sup>R. J. Bartlett and G. D. Purvis, *Int. J. Quantum Chem.* **14**, 561 (1978).
- <sup>40</sup>J. A. Pople, R. Krishnan, H. B. Schlegel, and J. S. Binkley, *Int. J. Quantum Chem.* **14**, 545 (1978).
- <sup>41</sup>J. A. Pople, M. Head-Gordon, and K. Raghavachari, *J. Chem. Phys.* **87**, 5968 (1987).
- <sup>42</sup>C. Møller and M. S. Plesset, *Phys. Rev.* **46**, 618 (1934).
- <sup>43</sup>J. A. Pople, R. Seeger, and R. Krishnan, *Int. J. Quantum Chem., Quantum Chem. Symp.* **11**, 149 (1977).
- <sup>44</sup>R. J. Bartlett, in *Annu. Rev. Phys. Chem.*, Vol. 32, edited by B. S. Rabinovitch, J. M. Schurr, and H. L. Strauss (Annual Reviews, Inc., Palo Alto, CA, 1981), p. 359.
- <sup>45</sup>J. A. Pople, J. S. Binkley, and R. Seeger, *Int. J. Quantum Chem., Quantum Chem. Symp.* **10**, 1 (1976).
- <sup>46</sup>R. Krishnan and J. A. J. A. Pople, *Int. J. Quantum Chem.* **14**, 91 (1978).
- <sup>47</sup>G. D. Purvis and R. J. Bartlett, *J. Chem. Phys.* **76**, 1910 (1982).
- <sup>48</sup>G. E. Scuseria and H. F. Schaefer, *J. Chem. Phys.* **90**, 3700 (1989).
- <sup>49</sup>G. E. Scuseria, C. L. Janssen, and H. F. Schaefer, *J. Chem. Phys.* **89**, 7382 (1988).
- <sup>50</sup>L. A. Curtiss, K. Raghavachari, G. W. Trucks, and J. A. Pople, *J. Chem. Phys.* **94**, 7221 (1991).
- <sup>51</sup>L. A. Curtiss, K. Raghavachari, P. C. Redfern, and J. A. Pople, *J. Chem. Phys.* **106**, 1063 (1997).
- <sup>52</sup>L. A. Curtiss, P. C. Redfern, K. Raghavachari, and J. A. Pople, *J. Chem. Phys.* **109**, 42 (1998).
- <sup>53</sup>L. A. Curtiss, K. Raghavachari, P. C. Redfern, and J. A. Pople, *J. Chem. Phys.* **112**, 7374 (2000).
- <sup>54</sup>G. S. Tschumper and H. F. Schaefer, *J. Chem. Phys.* **107**, 2529 (1997).
- <sup>55</sup>A. D. Becke, *Phys. Rev. A* **38**, 3098 (1988).
- <sup>56</sup>A. D. Becke, *J. Chem. Phys.* **98**, 5648 (1993).

- <sup>57</sup>C. Lee, W. Yang, and R. G. Parr, *Phys. Rev. B* **37**, 785 (1988).
- <sup>58</sup>C. Adamo and V. Barone, *J. Chem. Phys.* **108**, 664 (1998).
- <sup>59</sup>H. B. Schlegel, *J. Comput. Chem.* **3**, 214 (1982).
- <sup>60</sup>P. Csaszar and P. Pulay, *J. Mol. Struct.* **114**, 31 (1984).
- <sup>61</sup>H. Haberland, C. Ludewigt, H. G. Schindler, and D. R. Worsnop, *J. Chem. Phys.* **81**, 3742 (1984).
- <sup>62</sup>H. Haberland, H. G. Schindler, and D. R. Worsnop, *Ber. Bunsenges. Phys. Chem.* **88**, 270 (1984).
- <sup>63</sup>M. Armbruster, H. Haberland, and H. G. Schindler, *Phys. Rev. Lett.* **47**, 323 (1981).
- <sup>64</sup>C. G. Bailey, J. Kim, and M. A. Johnson, *J. Phys. Chem.* **100**, 16782 (1996).
- <sup>65</sup>P. Ayotte, G. H. Weddle, C. G. Bailey, M. A. Johnson, F. Vila, and K. D. Jordan, *J. Chem. Phys.* **110**, 6268 (1999).
- <sup>66</sup>J. Kim, I. Becker, O. Cheshnovsky, and M. A. Johnson, *Chem. Phys. Lett.* **297**, 90 (1998).
- <sup>67</sup>G. H. Lee, S. T. Arnold, J. G. Eaton, H. W. Sarkas, K. H. Bowen, C. Ludewigt, and H. Haberland, *Z. Phys. D: At., Mol. Clusters* **20**, 9 (1991).
- <sup>68</sup>J. V. Coe, G. H. Lee, J. G. Eaton, S. T. Arnold, H. W. Sarkas, K. H. Bowen, C. Ludewigt, H. Haberland, and D. R. Worsnop, *J. Chem. Phys.* **92**, 3980 (1990).
- <sup>69</sup>L. A. Posey, M. J. Deluca, P. J. Campagnola, and M. A. Johnson, *J. Phys. Chem.* **93**, 1178 (1989).
- <sup>70</sup>C. E. Klots, *J. Chem. Phys.* **71**, 4172 (1979).
- <sup>71</sup>T. Nagata, H. Yoshida, and T. Kondow, *Z. Phys. D: At., Mol. Clusters* **26**, 367 (1993).
- <sup>72</sup>T. Nagata, H. Yoshida, and T. Kondow, *Chem. Phys. Lett.* **199**, 205 (1992).
- <sup>73</sup>M. Saeki, T. Tsukuda, S. Iwata, and T. Nagata, *J. Chem. Phys.* **111**, 6333 (1999).
- <sup>74</sup>R. G. Keesee and A. W. Castleman, *J. Phys. Chem. Ref. Data* **15**, 1011 (1986).
- <sup>75</sup>A. W. Castleman and R. G. Keesee, *Annu. Rev. Phys. Chem.* **37**, 525 (1986).
- <sup>76</sup>J. G. Lahaye, R. Vandenhaute, and A. Fayt, *J. Mol. Spectrosc.* **123**, 48 (1987).